

A New Class of Iridium Complexes Suitable for Stepwise Incorporation into Linear Assemblies: Synthesis, Electrochemistry, and Luminescence

Victoria L. Whittle and J. A. Gareth Williams*

Department of Chemistry, University of Durham, Durham DH1 3LE, U.K.

Received September 11, 2007

A new family of cationic iridium(III) complexes is reported that contain two cyclometalating terdentate ligands. The complex $[\text{Ir}(\text{N}^{\wedge}\text{C}^{\wedge}\text{N-dpyx})(\text{N}^{\wedge}\text{N}^{\wedge}\text{C-phbpy})]^+$ (**1**) contains one $\text{N}^{\wedge}\text{C}^{\wedge}\text{N}$ -coordinating ligand, cyclometalating through the central phenyl ring, and one $\text{N}^{\wedge}\text{N}^{\wedge}\text{C}$ -coordinated ligand, cyclometalated at the peripheral phenyl ring [dpyxH = 1,3-di(2-pyridyl)-4,6-dimethylbenzene; phbpyH = 6-phenyl-2,2'-bipyridine]. This binding mode dictates a mutually *cis* arrangement of the cyclometalated carbon atoms: the complexes are thus bis-terdentate analogues of the well-known $[\text{Ir}(\text{N}^{\wedge}\text{C}^{\wedge}\text{ppy})_2(\text{N}^{\wedge}\text{N}^{\wedge}\text{bpy})]^+$ family of complexes, which similarly contain a *cis*- C_2N_4 coordination environment. The dpyx ligand can be brominated regioselectively at the carbon atom para to the metal under mild conditions. Starting from a modified complex, $[\text{Ir}(\text{N}^{\wedge}\text{C}^{\wedge}\text{N-dpyx})(\text{N}^{\wedge}\text{N}^{\wedge}\text{C-mtbp}\phi\text{-Br})]^+$ (**2**), which incorporates a pendent bromophenyl group, a sequential *cross-coupling*–*bromination*–*cross-coupling* strategy can be applied for the stepwise introduction of aryl groups into the ligands, using in situ palladium-catalyzed Suzuki reactions with arylboronic acids [mtbp ϕ -Br = 4-(*p*-bromophenyl)-6-(*m*-tolyl)bipyridine]. Dimetallic complexes **6** and **7** have similarly been prepared by a palladium-catalyzed reaction of complex **2** with 1,4-benzenediboronic acid and 4,4'-biphenyldiboronic acid, respectively. All five monometallic complexes and both dimetallic systems are luminescent in solution, emitting around 630 nm in MeCN at 298 K, with quantum yields in the range of 0.02–0.06, superior to $[\text{Ir}(\text{ppy})_2(\text{bpy})]^+$. The luminescence, electrochemistry, and singlet-oxygen-sensitizing abilities of the new family of complexes are discussed in the context of the tris-bidentate analogues and related bis-terdentate compounds that contain a *trans* arrangement of cyclometalated carbon atoms.

Introduction

The intense and sustained interest in $[\text{Ru}(\text{bpy})_3]^{2+}$, and its widespread application in studies of energy and electron transfer over the past 30 years, has been due to a combination of attractive properties.^{1–3} The lowest excited state has unambiguous triplet metal-to-ligand charge-transfer (³MLCT) character, with a lifetime sufficiently long for energy- and electron-transfer processes to compete with radiative and other nonradiative decay processes. Thermodynamically, the ³MLCT state is both strongly oxidizing and reducing, favoring light-induced electron-transfer processes. Biscyclometalated iridium(III) complexes such as $[\text{Ir}(\text{ppy})_2(\text{bpy})]^+$ ^{4,5} (Scheme 1) have excited-state properties quite similar to

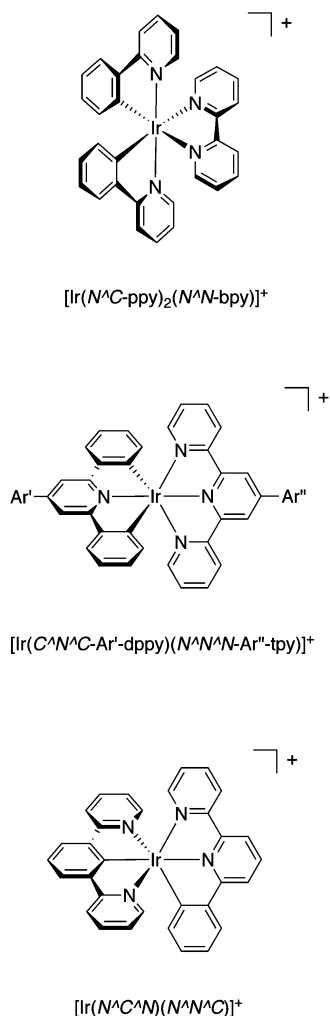
those of $[\text{Ru}(\text{bpy})_3]^{2+}$ and have been receiving increased attention over the past decade.^{6–9} They too have been studied as sensitizers of energy- and electron-transfer reactions.¹⁰ Although generally rather less brightly emissive than triscyclometalated complexes such as $[\text{Ir}(\text{ppy})_3]$,¹¹ their lumines-

* To whom correspondence should be addressed. E-mail: j.a.g.williams@durham.ac.uk.

- (1) Juris, A.; Balzani, V.; Barigelli, F.; Campagna, S. *Coord. Chem. Rev.* **1988**, *84*, 85.
- (2) Balzani, V. *Photochem. Photobiol. Sci.* **2003**, 459.
- (3) Vos, J. G.; Kelly, J. M. *Dalton Trans.* **2006**, 4869.
- (4) King, K. A.; Watts, R. J. *J. Am. Chem. Soc.* **1987**, *109*, 1589.

- (5) (a) Ohsawa, Y.; Sprouse, S.; King, K. A.; DeArmond, M. K.; Hanck, K. W.; Watts, R. J. *J. Phys. Chem.* **1987**, *91*, 1047. (b) Garces, F. O.; King, K. A.; Watts, R. J. *Inorg. Chem.* **1988**, *27*, 3464.
- (6) Dixon, I. M.; Collin, J.-P.; Sauvage, J.-P.; Flamigni, L.; Encinas, S.; Barigelli, F. *Chem. Soc. Rev.* **2000**, *29*, 385.
- (7) A comprehensive overview of the excited states of the different classes of iridium(III) complexes is provided by: (a) Flamigni, L.; Barbieri, A.; Sabatini, C.; Ventura, B.; Barigelli, F. *Top. Curr. Chem.* **2007**, *281*, 143.
- (8) Neve, F.; Crispini, A.; Campagna, S.; Serroni, S. *Inorg. Chem.* **1999**, *38*, 2250. (a) Neve, F.; Crispini, A.; Serroni, S.; Loiseau, F.; Campagna, S. *Inorg. Chem.* **2001**, *40*, 1093. (b) Neve, F.; La Deda, M.; Crispini, A.; Bellucci, A.; Puntoriero, F.; Campagna, S. *Organometallics* **2004**, *23*, 5856.
- (9) (a) Lepeltier, M.; Lee, T. K. M.; Lo, K. K. W.; Toupet, L.; Le Bozec, H.; Guerschais, V. *Eur. J. Inorg. Chem.* **2005**, 110. (b) Zhao, Q.; Liu, S.; Shi, M.; Wang, C.; Yu, M.; Li, L.; Li, F.; Yi, T.; Huang, C. *Inorg. Chem.* **2006**, *45*, 6152.

Scheme 1. Structures of Cationic Iridium Complexes Incorporating Two Metalated Carbon Atoms in the Coordination Sphere (N_4C_2 Coordination)^a



^a (a) The well-established tris-bidentate complexes [Ir(N^C)₂(N^N)]⁺, containing mutually cis-cyclometalated carbon atoms (top). (b) Scandola's bis-terdentate complexes containing dppy, with trans-disposed carbons (middle). (c) The generic structure of [Ir(C^N^N^C)(N^N^N^C)]⁺-coordinated complexes with cis-disposed carbons, the subject of the present work (bottom).

cence quantum yields are comparable to that of [Ru(bpy)₃]²⁺, and recent results have revealed their potential as emitters in electroluminescent devices.^{12,13} Other applications include the novel probes and sensors for biomolecules being pioneered by Lo and co-workers¹⁴ and emerging potential as photocatalysts for "water splitting" to generate hydrogen, recently demonstrated by Bernhard and co-workers.¹⁵

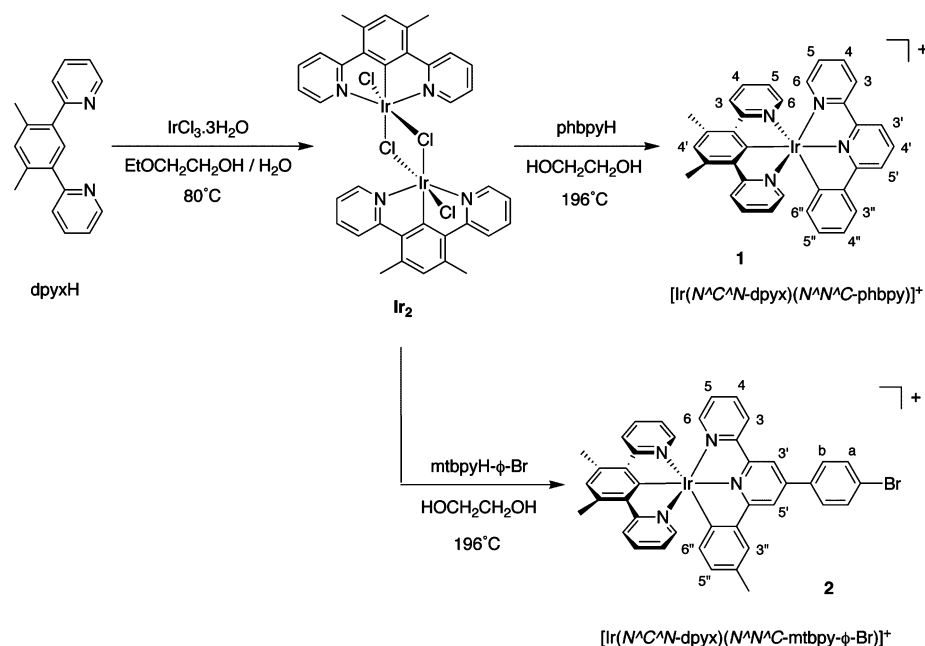
The intrinsic chirality of such *D*₃ and *C*₂ complexes means that they are normally isolated as racemic mixtures, resulting in the formation of stereoisomers when they are linked to form dyads or incorporated into donor–chromophore–acceptor

assemblies. These isomers are usually difficult to separate yet may display subtly different photophysical properties. Complexes containing two *terdentate* ligands, instead of three bidentate ones, are advantageous from this point of view, in that they are achiral with *D*_{2d} symmetry or lower; moreover, substitution at the central 4' position of the ligands allows *linear* rodlike extension.¹⁶ However, in ruthenium chemistry, complexes such as [Ru(tpy)₂]²⁺ are subject to severe non-radiative decay via low-lying, thermally populated metal-centered states, leading to very short excited-state lifetimes.¹⁷ Strategies attempting to overcome this problem have been reviewed recently by Medlycott and Hanan¹⁸ and include the use of modified terdentate ligands (e.g., cyclometalates,^{19,20} triazines,²¹ and six-membered chelating rings²²) all of which, however, tend to lower the MLCT energies.

In the case of iridium(III), the bis-terdentate complexes perhaps most closely analogous to [Ir(ppy)₂(bpy)]⁺ are those of the form [Ir(C^N^N^C-Ar'-dppy)(N^N^N-Ar''-tpy)]⁺ recently reported by Scandola et al. (Scheme 1; Ar'-dppy = 4-substituted 2,6-diphenylpyridine, Ar''-tpy = 4'-substituted terpyridine).^{23,24} However, these compounds have a mutually trans arrangement of the cyclometalated carbon atoms, as

- (11) For example, see: (a) Lamansky, S.; Djurovich, P. I.; Abdel-Razzaq, F.; Lee, H.; Adachi, C.; Burrows, P. E.; Forrest, S. R.; Thompson, M. E. *J. Am. Chem. Soc.* **2001**, *123*, 4304. (b) Lamansky, S.; Djurovich, P. I.; Murphy, D.; Abdel-Razzaq, F.; Kwong, R.; Tsyba, I.; Bortz, M.; Mui, B.; Bau, R.; Thompson, M. E. *Inorg. Chem.* **2001**, *40*, 1704. (c) Grushin, V. V.; Herron, N.; LeCloux, D. D.; Marshall, W. J.; Petrov, V. A.; Wang, Y. *Chem. Commun.* **2001**, 1494. (d) Tsuzuki, T.; Shirasawa, N.; Suzuki, T.; Tokito, S. *Adv. Mater.* **2003**, *15*, 1455. (e) Laskar, L. R.; Chen, T.-M. *Chem. Mater.* **2004**, *16*, 111.
- (12) (a) Slinker, J.; Bernards, D.; Houston, P. L.; Abruña, H. D.; Bernhard, S.; Malliaras, G. G. *Chem. Commun.* **2003**, 2392. (b) Slinker, J. D.; Gorodetsky, A. A.; Lowry, M. S.; Wang, J.; Parker, S.; Rohl, R.; Bernhard, S.; Malliaras, G. G. *J. Am. Chem. Soc.* **2004**, *126*, 2763.
- (13) Lowry, M. S.; Bernhard, S. *Chem.—Eur. J.* **2006**, *12*, 7970.
- (14) (a) Lo, K. K. W.; Hui, W. K.; Chung, C. K.; Tsang, K. H. K.; Ng, D. C. M.; Zhu, N. Y.; Cheung, K. K. *Coord. Chem. Rev.* **2005**, *249*, 1434. (b) Lo, K. K. W.; Hui, W. K.; Chung, C. K.; Tsang, K. H. K.; Lee, T. K. M.; Li, C. K.; Lau, J. S. Y.; Ng, D. C. M. *Coord. Chem. Rev.* **2006**, *250*, 1724. (c) Lo, K. K. W.; Lau, J. S. Y.; Lo, D. K. K.; Lo, L. T. L. *Eur. J. Inorg. Chem.* **2006**, 4054. (d) Lo, K. K. W.; Lau, J. S. Y. *Inorg. Chem.* **2007**, *46*, 700.
- (15) Lowry, M. S.; Goldsmith, J. I.; Slinker, J. D.; Rohl, R.; Pascal, R. A., Jr.; Malliaras, G. G.; Bernhard, S. *Chem. Mater.* **2005**, *17*, 5712.
- (16) A review of the concept is provided by: (a) Sauvage, J.-P.; Collin, J.-P.; Chambron, J.-C.; Guillerez, S.; Coudret, C.; Balzani, V.; Barigelli, F.; De Cola, L.; Flamigni, L. *Chem. Rev.* **1994**, *94*, 993.
- (17) Winkler, J. R.; Netzel, T. L.; Creutz, C.; Sutin, N. *J. Am. Chem. Soc.* **1987**, *109*, 2381. (a) Pyo, S.; Pérez-Cordero, E.; Bott, S. G.; Echegoyen, L. *Inorg. Chem.* **1999**, *38*, 3337.
- (18) Medlycott, E. A.; Hanan, G. S. *Chem. Soc. Rev.* **2006**, 250, 1763.
- (19) (a) Collin, J.-P.; Beley, M.; Sauvage, J.-P.; Barigelli, F. *Inorg. Chim. Acta* **1991**, *186*, 91. (b) Barigelli, F.; Ventura, B.; Collin, J.-P.; Kayhanian, R.; Gaviña, P.; Sauvage, J.-P. *Eur. J. Inorg. Chem.* **2000**, 113.
- (20) (a) Constable, E. C.; Hannon, M. J. *Inorg. Chim. Acta* **1993**, *211*, 101. (b) Constable, E. C.; Cargill Thompson, A. M. W.; Cherryman, J.; Liddiment, T. *Inorg. Chim. Acta* **1995**, *235*, 165. (c) Bardwell, D. A.; Cargill Thompson, A. M. W.; Jeffery, J. C.; McCleverty, J. A.; Ward, M. D. *J. Chem. Soc., Dalton Trans.* **1996**, 873.
- (21) (a) Polson, M. I. J.; Taylor, N. J.; Hanan, G. S. *Chem. Commun.* **2002**, 1356. (b) Polson, M. I. J.; Medlycott, E. A.; Hanan, G. S.; Mikelson, L.; Taylor, N. J.; Watanabe, M.; Tanaka, Y.; Loiseau, F.; Passalacqua, R.; Campagna, S. *Chem.—Eur. J.* **2004**, *10*, 3640.
- (22) (a) Abrahamsson, M.; Wolpher, H.; Johansson, O.; Larsson, J.; Kritikos, M.; Eriksson, L.; Norrby, P.-O.; Bergquist, J.; Sun, L.; Åkermar, B.; Hammarström, L. *Inorg. Chem.* **2005**, *44*, 3215. (b) Abrahamsson, M.; Jäger, M.; Österman, T.; Eriksson, L.; Persson, P.; Becker, H.-C.; Johansson, O.; Hammarström, L. *J. Am. Chem. Soc.* **2006**, *128*, 12616.

- (10) (a) Ortman, I.; Didier, P.; Kirsch-De Mesmaecker, A. *Inorg. Chem.* **1995**, *35*, 3695. (b) van Diemen, J. H.; Hage, R.; Haasnoot, J. G.; Lempers, H. E. B.; Reedijk, J.; Vos, J. G.; De Cola, L.; Barigelli, F.; Balzani, V. *Inorg. Chem.* **1992**, *31*, 3518. (c) Serroni, S.; Juris, A.; Campagna, S.; Venturi, M.; Denti, G.; Balzani, V. *J. Am. Chem. Soc.* **1994**, *116*, 9086. (d) Sabatini, C.; Barbieri, A.; Barigelli, F.; Arm, K. J.; Williams, J. A. G. *Photochem. Photobiol. Sci.* **2007**, *6*, 397. (e) Welter, S.; Lafolet, F.; Cecchetto, E.; Vergeer, F.; De Cola, L. *ChemPhysChem* **2005**, *6*, 2417.

Scheme 2. Synthesis of **1** via the Chloro-Bridged Dimer **Ir₂**

opposed to the *cis* disposition normally observed in the bidentate systems; density functional theory (DFT) calculations reveal clear-cut localization of the highest occupied molecular orbital (HOMO) on the dppy and the lowest unoccupied molecular orbital (LUMO) on the tpy ligand, and hence an excited state of predominant ligand-to-ligand CT (LLCT) nature, characterized by a low radiative rate constant. Earlier, using more conjugated quinolyl ligands, Mamo et al. isolated an interesting homoleptic iridium complex containing two $\text{N}^{\wedge}\text{N}^{\wedge}\text{C}$ -coordinating 2,6-(2'-quinolynyl)pyridine ligands, which emits from a $^3\text{MLCT}$ state.^{25,26} Complexes containing one terdentate cyclometalating ligand and one bidentate cyclometalating ligand, some of which are strongly emissive, have also been recently reported by Haga and co-workers.²⁷ In these cases, the sixth site is occupied by a monodentate ligand such as chloride.

In this contribution, we describe the synthesis and properties of a simple bis-terdentate iridium complex containing *cis*-disposed cyclometalated carbon atoms, of the generic type represented in Scheme 1c and analogous to the popular $[\text{Ir}(\text{ppy})_2(\text{bpy})]^+$ systems. We show that complexes based on this core structure are amenable to facile, *in situ* elaboration along the principal axis of the molecule, in a stepwise manner, using palladium-catalyzed cross-coupling reactions, making them potentially ideal as versatile units for incorporation into linear photoactive assemblies.

Results and Discussion

1. Strategy. Previously, we showed that 1,3-di(2-pyridyl)-4,6-dimethylbenzene (**dpyxH**) can bind symmetrically to iridium in an $\text{N}^{\wedge}\text{C}^{\wedge}\text{N}$ manner.²⁸ Substituents at the C4 and C6 positions were required to prevent competitive C4 cyclometalation leading to bidentate $\text{N}^{\wedge}\text{C}$ coordination. Thus, the reaction of **dpyxH** with iridium trichloride generates the chloro-bridged dimeric product $[\text{Ir}(\text{N}^{\wedge}\text{C}^{\wedge}\text{N-dpyx})\text{Cl}(\mu\text{-Cl})_2]$ (denoted **Ir₂**; Scheme 2), from which the complex $[\text{Ir}(\text{N}^{\wedge}\text{C}^{\wedge}\text{N-dpyx})(\text{C}^{\wedge}\text{N}^{\wedge}\text{C-dppy})]$ could be prepared, containing three cyclometalated carbon atoms in the coordination sphere of the metal.²⁹ Despite displaying attractive luminescence properties ($\lambda_{\text{max}} = 585 \text{ nm}$, $\phi = 0.21$, and $\tau = 3.9 \mu\text{s}$ in MeCN), this complex proved to be unstable in solution with respect to photodissociation of one of the two mutually trans-cyclometalated carbons, effectively ruling out further derivatization. In the present work, we sought to use the same intermediate, **Ir₂**, to obtain a cationic complex containing two *cis*-cyclometalating carbon atoms, and to explore the possibility of elaborating it further *in situ*, using palladium-catalyzed cross-coupling reactions.

2. Synthesis of Parent Complex 1. The reaction of the dimer **Ir₂** with 6-phenyl-2,2'-bipyridine (**phbpyH**) in ethylene glycol at 196°C , followed by ion exchange with KPF_6 and chromatographic purification on silica, gave $[\text{Ir}(\text{N}^{\wedge}\text{C}^{\wedge}\text{N-dpyx})(\text{N}^{\wedge}\text{N}^{\wedge}\text{C-phbpy})](\text{PF}_6)$ (**1**) as a yellow/orange solid (Scheme 2). Complex **1** is the first example of a new family of heteroleptic iridium complexes comprising two different terdentate, cyclometalating ligands. Evidence for cyclometalation of the 6-phenylbipyridine ligand is provided by the ^1H NMR spectrum, which shows a very low-frequency

(23) Polson, M.; Fracasso, S.; Bertolasi, V.; Ravaglia, M.; Scandola, F. *Inorg. Chem.* **2004**, *43*, 1950.

(24) Polson, M.; Ravaglia, M.; Fracasso, S.; Garavelli, M.; Scandola, F. *Inorg. Chem.* **2005**, *44*, 1282.

(25) Mamo, A.; Steflo, I.; Parisi, M. F.; Credi, A.; Venturi, M.; Di Pietro, C.; Campagna, S. *Inorg. Chem.* **1997**, *36*, 5947.

(26) Di Marco, G.; Lanza, M.; Mamo, A.; Steflo, I.; Di Pietro, C.; Romeo, G.; Campagna, S. *Anal. Chem.* **1998**, *70*, 5019.

(27) (a) Yutaka, T.; Obara, S.; Ogawa, S.; Nozaki, K.; Ikeda, N.; Ohno, T.; Ishii, Y.; Sakai, K.; Haga, M.-A. *Inorg. Chem.* **2005**, *44*, 4737. (b) Obara, S.; Itabashi, M.; Okuda, F.; Tamaki, S.; Tanabe, Y.; Ishii, Y.; Nozaki, K.; Haga, M. A. *Inorg. Chem.* **2006**, *45*, 8907.

(28) Wilkinson, A. J.; Goeta, A. E.; Foster, C. E.; Williams, J. A. G. *Inorg. Chem.* **2004**, *43*, 6513.

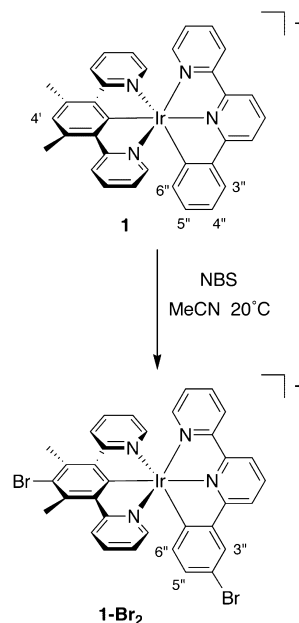
(29) Wilkinson, A. J.; Puschmann, H.; Howard, J. A. K.; Foster, C. E.; Williams, J. A. G. *Inorg. Chem.* **2006**, *45*, 8685.

doublet at 5.94 ppm coupled to a second doublet at 6.62 ppm, each with an integral of one. These signals are assigned to $H^{6''}$ and $H^{5''}$, respectively (see Scheme 2 for the atom-numbering system employed). In cyclometalated complexes of arylpyridine ligands, low-frequency/high-field shifts are typically characteristic of protons adjacent to the site of cyclometalation. In the present case, the effect is augmented by the protons being positioned above the plane of the central aryl ring of the $N^{\wedge}C^{\wedge}N$ -coordinating ligand, an environment in which they will experience an upfield shift, owing to the diamagnetic ring current associated with the latter. The isolation of the cyclometalated $N^{\wedge}N^{\wedge}C$ -coordination mode of phbpy with iridium(III) contrasts with the result obtained upon the reaction of phbpyH with $[\text{Ir}(N^{\wedge}N^{\wedge}N\text{-tpy})\text{Cl}_3]$, which, under similar reaction conditions, led only to bidentate $N^{\wedge}N$ coordination to give $[\text{Ir}(N^{\wedge}N^{\wedge}N\text{-tpy})(N^{\wedge}N\text{-phbpy-H})\text{Cl}]^{2+}$.³⁰

3. Bromination of 1. We previously demonstrated that biscyclometalated, tris-bidentate complexes of the type $[\text{Ir}(\text{ppy})_2(\text{bpy})]^+$ are susceptible to facile electrophilic bromination of the cyclometalating phenyl rings, which occurs selectively at the positions para to the metal ion.^{31,32} This allows such complexes to be activated to subsequent cross-coupling reactions, offering a versatile, stepwise route to multimetallic complexes. This remarkable reactivity, similar to that observed for $[\text{Ru}(\text{bpy})_2(\text{ppy})]^+$ by Coudret et al.,³³ can be attributed to the increase in the electron density in the phenyl rings that accompanies cyclometalation.

With a view to developing a pathway for linear elaboration of the new $[\text{Ir}(N^{\wedge}C^{\wedge}N)(N^{\wedge}N^{\wedge}C)]^+$ complexes, the reactivity of **1** with respect to bromination was investigated. A solution of **1** in an acetonitrile solution was treated with 1 equiv of *N*-bromosuccinimide (NBS) at room temperature, and the evolution of the ^1H NMR spectrum was followed. The characteristic singlet resonances of the $H^{4'}$ proton of dpyx at 7.21 ppm and of the two degenerate methyl groups at 2.97 ppm declined over a period of several hours, accompanied by the growth of a new methyl singlet at 3.19 ppm (data in acetone- d_6). These changes are consistent with bromination at $C^{4'}$ of dpyx (Scheme 3). The resonances of the protons of the phbpy ligand also underwent substantial changes, suggesting that bromination was occurring simultaneously at $C^{4''}$ of phbpy. Indeed, the dibrominated complex (**1-Br₂**; Scheme 3) could be obtained in essentially quantitative yield upon the addition of a second 1 equiv of NBS. While the rate of bromination appeared to be a little faster for the dpyx ligand, the relative rates proved to be too similar for selective bromination of this ligand to be achieved using just 1 equiv of NBS. Despite the widespread use of NBS in organic chemistry for benzylic bromination, it should be noted that no bromination of the methyl groups of dpyx was observed. This selectivity stems from the mild

Scheme 3. Treatment of the Parent Complex **1** with NBS in MeCN at Room Temperature Leading to Bromination of Both of the Cyclometalated Rings at the Position Para to the Metal, **1-Br₂**



conditions employed because radical benzylic bromination normally requires elevated temperatures.

Interestingly, the ligand 1-bromo-3,5-di(2-pyridyl)-2,6-dimethylbenzene, which is formed in situ in the above bromination reaction, appears to be an elusive compound as the “free” ligand. In an attempt to synthesize it, 1,3,5-tribromo-2,6-dimethylbenzene was prepared by bromination of 3,5-dimethylaniline, followed by deamination via the diazonium salt, and then subjected to palladium-catalyzed Stille cross-coupling with 2-tri-*n*-butylstannylpyridine. Using 2 equiv of the stannane, the only product formed in significant amounts was the singly reacted compound 1,3-dibromo-5-pyridyl-2,6-dimethylbenzene. Further reaction with more stannane proceeds more slowly and, surprisingly, the rate of cross-coupling at the 1 position proves to be comparable, and indeed slightly faster, than that at the 3 position. The two dipyrindyl isomers that form cannot be readily separated by chromatography or crystallization. The tripyridyl compound, on the other hand, could be obtained in good yield (see the Supporting Information).

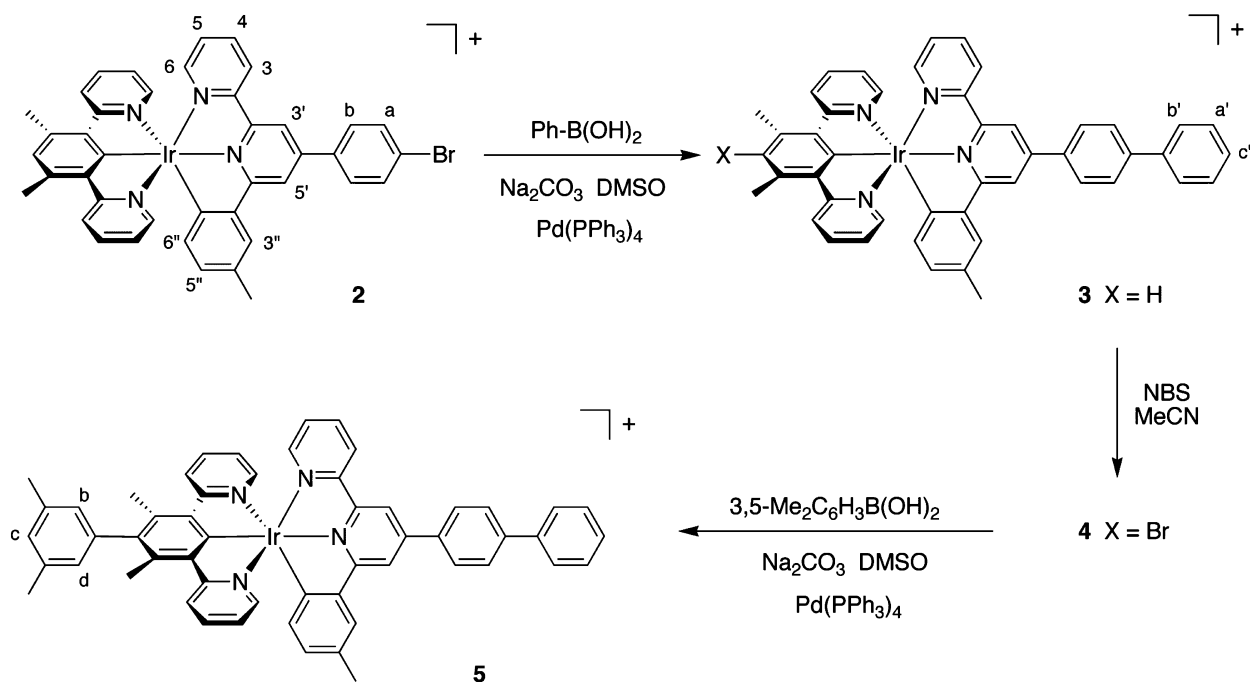
4. Synthesis of Modified Complex 2. In order to achieve the goal of stepwise elaboration of the $[\text{Ir}(N^{\wedge}C^{\wedge}N)(N^{\wedge}N^{\wedge}C)]^+$ system specifically along the principal axis [i.e., the $C^{4'}_{\text{dpyx}}\text{—Ir—}C^{4''}_{\text{phbpy}}$ axis, which is the equivalent of the C_2 axis of bis(terpyridyl) complexes], the competitive bromination of the cyclometalating ring of phbpy must be blocked, while a means for functionalization of this ligand along the axis must be introduced. Complex **2** (Scheme 2) was identified as an appropriate target for this purpose. The new ligand 4-(*p*-bromophenyl)-6-(*m*-tolyl)bipyridine (mtbpyH- ϕ -Br) was synthesized in adequate yield by a modified Kröhnke procedure, in which the initial aldol reaction of *m*-methylacetophenone with *p*-bromobenzaldehyde and the subsequent Michael reaction with 2-acetylpyridine were carried out under solvent-free conditions (reaction scheme and experimental

(30) Bexon, A. J. S.; Williams, J. A. G. *C. R. Chimie* **2005**, *8*, 1326.

(31) Arm, K. J.; Williams, J. A. G. *Chem. Commun.* **2005**, 230.

(32) Arm, K. J.; Williams, J. A. G. *Dalton Trans.* **2006**, 2172.

(33) Coudret, C.; Frayssé, S.; Launay, J.-P. *Chem. Commun.* **1998**, 663.
Frayssé, S.; Coudret, C.; Launay, J.-P. *J. Am. Chem. Soc.* **2003**, *125*, 5880.

Scheme 4. Sequential Cross-Coupling–Bromination–Cross-Coupling Reactions on the Modified Complex **2**, Leading to Complexes **3–5**, Respectively

details are provided in the Supporting Information).³⁴ This ligand reacts with the iridium dimer **Ir**₂ under the same conditions as phbpyH to generate [Ir(N[^]C[^]N-dpyx)(N[^]N[^]C-mtbp-*φ*-Br)](PF₆) (**2**; Scheme 2), in which cyclometalation of mtbp-*φ*-Br occurs exclusively at the position para to the methyl group. The isolated yield is high (84%), and there is no evidence for the formation of the alternative isomer comprising metalation ortho to the methyl group, which is presumably disfavored on both steric and electronic grounds.

5. Sequential Cross-Coupling Reactions of Complex 2. Previously, we showed that bromo-substituted bis(terpyridyl) ruthenium(II) and -iridium(III) complexes can undergo palladium-catalyzed Suzuki cross-coupling reactions with arylboronic acids to generate compounds with more elaborate ligands in situ.^{32,35,36} When similar conditions are applied in the present instance, complex **2** was found to undergo smooth cross-coupling with phenylboronic acid in a dimethyl sulfoxide solution, in the presence of sodium carbonate as the base and using the conventional catalyst Pd(PPh₃)₄, to generate **3** (Scheme 4), which incorporates a biphenyl pendent on the N[^]N[^]C ligand. Complex **3** was isolated in good yield after precipitation of the hexafluorophosphate salt and chromatographic purification, with the main side product being a trace of the debrominated complex.

Treatment of a solution of complex **3** in an acetonitrile solution with NBS at room temperature led to bromination specifically at the C^{4'} position of dpyx, as revealed by the

disappearance of the H^{4'} resonance in the ¹H NMR spectrum and an accompanying shift of the dpyx methyl singlet from 2.98 to 3.22 ppm (in acetone-*d*₆). The new bromo-functionalized complex **4** (Scheme 4) is now primed for further cross-coupling reactions but, in this case, on the N[^]C[^]N ligand. We selected 3,5-dimethylbenzeneboronic acid to explore this possibility, which readily underwent cross-coupling under the same conditions as those used in the conversion of **2** → **3** {Na₂CO₃, Pd(PPh₃)₄, dimethyl sulfoxide, 80 °C}. Apparently, the steric hindrance expected to be associated with the two methyl groups flanking the C–Br bond of **4** does not significantly impede the cross-coupling reaction nor necessitate the use of stronger bases as is sometimes observed for coupling of sterically hindered partners in purely organic systems.³⁸ In the resulting product **5**, the main change in the ¹H NMR spectrum compared to **4** is the appearance of three new singlets in the aromatic region. The inequivalence of the two protons ortho to the aryl–aryl bond (i.e., H^b and H^d in structure **5**, Scheme 4) arises from the lack of rotation about this bond due to the flanking methyl groups on the dpyx unit. This leads to the pendent ring being positioned in a plane that is essentially orthogonal to the plane of dpyx. Protons H^b and H^d of dpyx are then clearly in different environments with respect to the asymmetric N[^]N[^]C-coordinating phbpy ligand: as represented in Scheme 4, H^b is in line with the pyridyl ring of phbpy, whereas H^d is on the side of the phenyl ring. Variable-temperature ¹H NMR experiments in dimethyl-*d*₆ sulfoxide revealed no evidence of the onset of rotation about the aryl–aryl bond, even at 363 K. In fact, the barrier to rotation in 2,6-dimethylbiphenyl

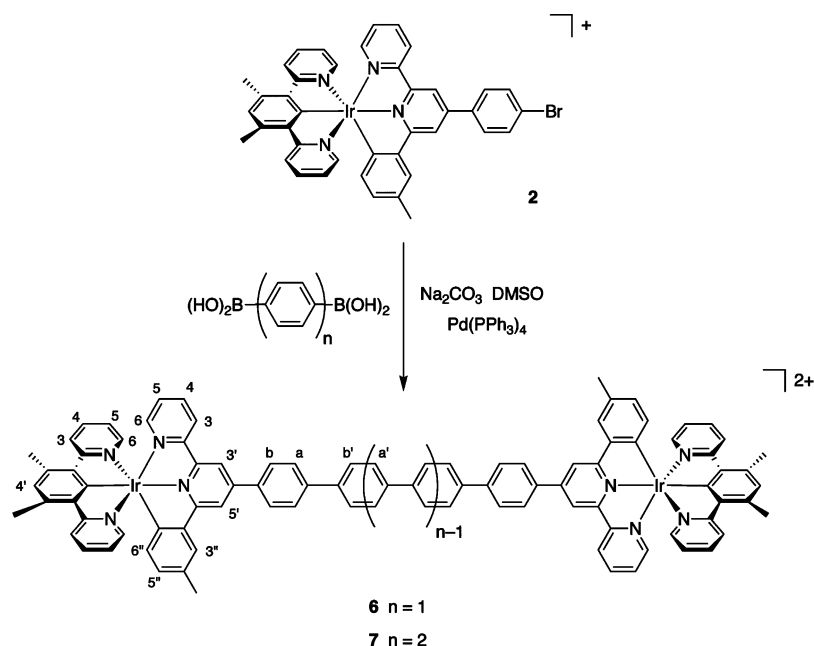
(34) Cave, G. W. V.; Raston, C. L. *Chem. Commun.* **2000**, 2199.

(35) Aspley, C. J.; Williams, J. A. G. *New J. Chem.* **2001**, 25, 1136.

(36) Leslie, W.; Batsanov, A.; Howard, J. A. K.; Williams, J. A. G. *Dalton Trans.* **2004**, 623.

(37) Ren and co-workers have also employed in situ Suzuki and Sonogashira reactions recently to build up metal complexes, in their case, on diarylformamidinate-bridged diruthenium compounds: (a) Xu, G.-L.; Ren, T. *Inorg. Chem.* **2006**, 45, 10449. (b) Chen, W. Z.; Ren, T. *Inorg. Chem.* **2006**, 45, 9175.

(38) Watanabe, T.; Miyaura, N.; Suzuki, A. *Synlett* **1992**, 207.

Scheme 5. Synthesis of the Dinuclear Complexes **6** and **7** by Cross-Coupling of **2** with Aryldiboronic Acids

has been estimated to exceed 100 kJ mol^{-1} ,³⁹ which compares to a value of only 3 kJ mol^{-1} for *RT* at 363 K.

6. Dimetallic Assemblies. The potential of the complexes for incorporation into multimetallic assemblies has been assessed in a preliminary study. Complex **2** was cross-coupled with 1,4-benzenediboronic acid, using a molar ratio of approximately 2:1 (complex–diboronic acid). The reaction proceeded readily, under the same conditions as those described in the preceding section for elaboration of **2** with arylboronic acids, to give the dimetallic assembly $[\{\text{Ir}(\text{dpix})_2\}_2\mu\text{-(mtbpy-}\phi_3\text{-mtbpy)}]^{2+}$ (**6**), in which the constituent iridium complexes are effectively connected by a bridge of three phenyl rings (Scheme 5). An analogous reaction with 4,4'-biphenyldiboronic acid led to the corresponding assembly $[\{\text{Ir}(\text{dpix})_2\}_2\mu\text{-(mtbpy-}\phi_4\text{-mtbpy)}]^{2+}$ (**7**), with a four-ring bridge. Homometallic dimers (dyads) of the elements ruthenium(II), osmium(II), and iridium(III) bound to polypyridyl ligands and bridged by poly(phenylene) linkers have been the subject of much research interest over the past 20 years.^{40,41} Those based on tris-bidentate systems, such as the $[\{\text{Ir}(\text{ppy})_2\}_2\mu\text{-(bpy-}\phi\text{-bpy)}]^{2+}$ analogues of **6** and **7**,⁴¹ are necessarily formed, as noted in the introduction, as diastereomeric mixtures of two pairs of enantiomers, whereas single products are isolated in the present instance, which makes use of bis-terdentate metal centers. Somewhat related dimers of the form $\{\text{Ir}(\text{dpix})\}_2\mu\text{-(tpy-}\phi_n\text{-tpy)}]^{4+}$ ($n = 0\text{--}3$) have been reported recently by Collin et al., prepared using preformed bridging terpyridine ligands.⁴²

7. Electrochemistry. All five of the new monometallic complexes display at least two reversible or quasi-reversible

electrochemical processes within the range of -2.0 to $+1.5$ V in an acetonitrile solution. The cyclic voltammogram of complex **1** (Figure 1) is representative in the profile of all of the complexes. A one-electron-reduction process, which occurs at -1.39 V vs SCE in the case of **1** (Table 1), is assigned to the reduction of the $\text{N}^{\wedge}\text{N}^{\wedge}\text{C}$ ligand on several grounds. First, the value is close to the reduction potential of -1.35 V observed for the analogous tris-bidentate complex, $[\text{Ir}(\text{ppy})_2(\text{bpy})]^+$, where reduction is unambiguously centered on the bipyridine ligand. In complex **1**, the reduction is likely to be centered on the bipyridyl fragment of the $\text{N}^{\wedge}\text{N}^{\wedge}\text{C}$ ligand, with the phenyl ring in the 6 position having only a small influence. Second, the value is mildly displaced to more negative potentials compared to that of Scandola's $[\text{Ir}(\text{dppy})(\text{tpy})]^+$ complexes (E° of ca. -1.27 V vs SCE),

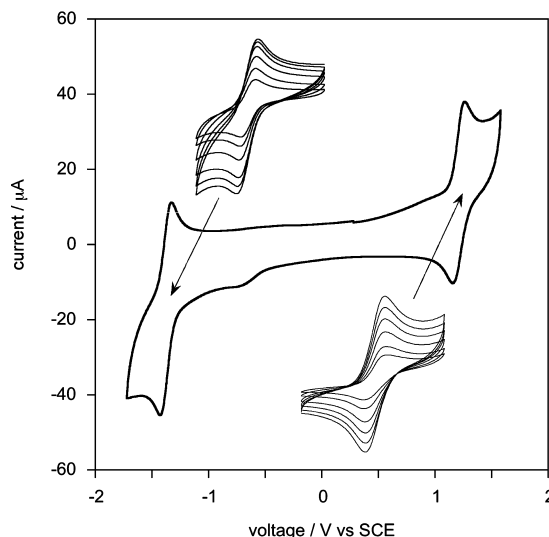


Figure 1. Cyclic voltammogram of **1** in an acetonitrile solution at 298 K, in the presence of 0.1 M Bu_4NBF_4 as the supporting electrolyte, at a scan rate of 300 mV s^{-1} . The insets show the first oxidation and first reduction at a series of scan rates (50, 100, 200, 300, 400, and 500 mV s^{-1}); the current varies linearly with the square root of the scan rate.

(39) Grumadas, A. J.; Poshkus, D. P.; Kiselev, A. V. *J. Chem. Soc., Faraday Trans.* **1982**, 78, 2013.

(40) Welter, S.; Salluce, N.; Belser, P.; Groeneveld, M.; De Cola, L. *Coord. Chem. Rev.* **2005**, 249, 1360.

(41) Lafalet, F.; Welter, S.; Popovic, Z.; De Cola, L. *J. Mater. Chem.* **2005**, 15, 2820.

(42) Auffrant, A.; Barbieri, A.; Barigelletti, F.; Collin, J.-P.; Flamigni, L.; Sabatini, C.; Sauvage, J.-P. *Inorg. Chem.* **2006**, 45, 10990.

Table 1. Ground-State UV–Visible Absorption and Electrochemical Data of the Iridium Complexes in CH₃CN at 298 K

complex ^a	absorbance $\lambda_{\text{max}}/\text{nm}$ ($\epsilon/\text{M}^{-1} \text{ cm}^{-1}$)	$E_{1/2}^{\text{ox}}/\text{V}$ ($\Delta E/\text{mV}$) ^b	$E_{1/2}^{\text{red}}/\text{V}$ ($\Delta E/\text{mV}$) ^b
[Ir(ppy) ₂ (bpy)] ⁺	255 (46 600), 303 (22 400), 334 (9210), 370 (6160), 405 (3710), 465 (720)	1.28 ^c	−1.35 ^c
[Ir(tddpy)(tpy- <i>φ</i> -Br)] ⁺ ^d	283 (86 300), 323 sh (53 700), 437 (15 000), 482 sh (10 900), 514 (9200)	1.08 (90)	−1.24 (95)
[Ir(dpyx)(phbpy)] ⁺ (1)	240 (24 500), 265 (22 100), 294 sh (16 600), 367 (5360), 411 (5490), 479 (640)	1.21 (83)	−1.39 (86)
[Ir(dpyx)(mtbpy- <i>φ</i> -Br)] ⁺ (2)	232 (61 700), 242 (61 600), 284 (65 150), 372 (17 870), 411 sh (12 100), 479 (1800)	1.22 (80)	−1.15 (100)
[Ir(dpyx)(mtbpy- <i>φ</i> -Ph)] ⁺ (3)	232 (65 300), 293 (60 900), 375 (23 200), 412 sh (13 200), 479 (1940)	0.96 (90)	−1.54 (80)
[Ir(Brdpyx)(mtbpy- <i>φ</i> -Ph)] ⁺ (4)	235 (58 000), 286 (50 700), 376 (16 360), 425 (8160), 483 (1600)	0.94 (100)	−1.82 (100)
[Ir(Me ₂ -C ₆ H ₃ -dpyx)(mtbpy- <i>φ</i> -Ph)] ⁺ (5)	229 (149 000), 273 sh (122 000), 293 (136 000), 375 (47 500), 420 (23 400), 481 (4160)	0.89 (90)	−1.66 (90)
[{Ir(dpyx) ₂ }] ₂ μ-(mtbpy- <i>φ</i> -3-mtbpy)] ²⁺ (6)	233 (86 300), 275 (63 500), 292 (67 400), 320 (64 600), 379 (51 800), 479 (32 500)	0.84 (100)	−1.85 ^e (100)
[{Ir(dpyx) ₂ }] ₂ μ-(mtbpy- <i>φ</i> -4-mtbpy)] ²⁺ (7)	232 (71 100), 287 (74 100), 320 (77 000), 377 (61 000), 479 (33 380)	1.01 (140)	−1.72 ^e (130)

^a Hexafluorophosphate salts in each case. ^b Using Bu₄NPF₆ (0.1 M) as the supporting electrolyte; values are at scan rate 300 mV s^{−1} (except for **5**, at 50 mV s^{−1}) and are reported relative to SCE, measured using ferrocene as the standard ($E_{1/2}^{\text{ox}} = 0.42 \text{ V}$ vs SCE). ^c In DMF solution, data from ref 5a. ^d Data from refs 23 and 24. ^e Reduction waves were poorly defined for the dimetallic systems, and a more detailed study was hampered by their poor solubility in MeCN.

where a clear-cut reduction on the terpyridine ligand is assigned. That a change from bipyridine to terpyridine has a small stabilizing influence on the reduction is well established, for example, from the reduction potentials of [Ir(bpy)₃]³⁺ and [Ir(tpy)₂]³⁺ ($E^{\circ} = -1.0$ and -0.77 V vs SCE, respectively^{43,44}). Finally, DFT studies carried out using the methods described previously²⁹ reveal that the LUMO is almost exclusively localized on the bipyridyl fragment of the N[^]C[^]N[^]C ligand (see the Supporting Information for plots of the frontier orbitals).

At positive potentials, there is a reversible one-electron oxidation, occurring at 1.21 V for **1**, which is similar to the value of 1.28 V observed in the tris-bidentate analogue [Ir(ppy)₂(bpy)]⁺. As has been noted elsewhere,^{6,23,24,45} the strong covalent character of the Ir–C bonds in the cyclometalated complexes means that the oxidation wave cannot be assigned simply to metal-centered oxidation, and indeed the DFT calculations confirm that the HOMO is delocalized over the metal and the cyclometalating ring of the N[^]C[^]N[^]C ligand. The values of 1.21 and 1.28 V for these complexes containing cis-disposed carbon atoms are somewhat higher than the values observed for Scandola's series of [Ir(dp-*py*)(tpy)]⁺ complexes in which there is a trans arrangement of the two carbon atoms. This is in line with studies of the *fac* and *mer* isomers of [Ir(ppy)₃], which show that the *mer* isomers, having a trans disposition of two of the carbon atoms, are more readily oxidized than the *fac* isomers by about 0.1 V.

The introduction of the pendent *p*-bromophenyl group onto the N[^]C[^]N[^]C ligand is seen to facilitate reduction by 240 mV, which can be attributed to a net electron-withdrawing effect and more extended conjugation introduced into the N[^]C[^]N[^]C ligand, upon which the LUMO is localized. On the other hand, further extension to a biphenyl pendent shifts $E_{1/2}^{\text{red}}$ to more negative potentials, so the net effect in this case must be one of electron donation through the π -bonding frame-

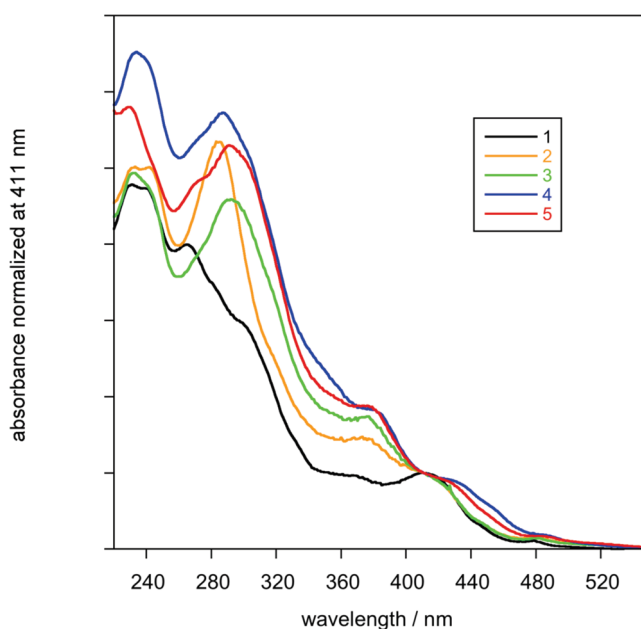


Figure 2. Absorption spectra of the new [Ir(N[^]C[^]N[^]C)(N[^]C[^]N[^]C)]⁺ iridium complexes **1–5** in an acetonitrile solution at 298 K, normalized at 411 nm to aid comparison.

work. This is also manifest in the decreased oxidation potential of this complex, with $E_{1/2}^{\text{ox}}$ being shifted by 250 mV to less positive potential compared to **1**. Meanwhile, substituents on the N[^]C[^]N[^]C ligand also stabilize slightly the oxidation while destabilizing the reduction (Table 1).

8. Ground-State UV–Visible Absorption. The absorption spectra of all of the complexes in an acetonitrile solution at room temperature show very intense broad bands in the region between 220 and 330 nm (Figure 2 and Table 1). By comparison with the literature data for biscyclometalated cationic iridium complexes, these are assigned to spin-allowed $^1\pi\text{--}\pi^*$ transitions of the ligands. A notable difference between the derivative **2** and parent complex **1** is the appearance of a relatively sharp and well-defined band centered at 285 nm, which must be associated with the introduction of the pendent aryl unit. This feature persists in complexes **3–5**. A similar band centered around 280 nm was previously observed in [Ir(tpy)₂]³⁺ complexes bearing

(43) Kahl, J. A.; Hanck, K. W.; DeArmond, K. *J. Phys. Chem.* **1978**, *82*, 540.

(44) Collin, J.-P.; Dixon, I. M.; Sauvage, J.-P.; Williams, J. A. G.; Barigelletti, F.; Flamigni, L. *J. Am. Chem. Soc.* **1999**, *121*, 5009.

(45) Hay, P. J. *J. Phys. Chem. A* **2002**, *106*, 1634.

biphenyl pendants.³⁶ A series of bands in the region 330–450 nm are attributable to spin-allowed CT transitions, the lowest of which is well-resolved in **1** (411 nm) but less so in **2–5** because of increased absorption around 375 nm. In each complex, there is also a weak, low-energy band ca. 480 nm, likely to be due to direct absorption to the lowest-energy triplet state facilitated by the high spin–orbit coupling constant of the iridium center ($\zeta = 3909 \text{ cm}^{-1}$ ⁴⁶). Both of the latter bands (i.e., those at ca. 411 and 480 nm) are slightly red-shifted in complexes **4** and **5** but not in **2** and **3**, suggesting that their energy is influenced primarily by the N^{^C^N} ligand substitution.

While the positions of the bands are roughly comparable to those displayed by $[\text{Ir}(\text{ppy})_2(\text{bpy})]^+$ (Table 1), the spectra are quite different from those of the trans-cyclometalated complexes $[\text{Ir}(\text{C}^{\wedge}\text{N}^{\wedge}\text{C}-\text{Ar}'\text{-dppy})(\text{N}^{\wedge}\text{N}^{\wedge}\text{N}-\text{Ar}''\text{-tpy})]^+$, which show intense bands extending to much lower energy^{23,24} (longest wavelength band around 514 nm with $\epsilon \sim 9000$; Table 1). In that case, DFT calculations revealed a HOMO comprising both metal and dppy character and a tpy-localized LUMO as in the present instance, where the LUMO is localized on the bpy moiety of the N^{^C^N} ligand as described above. The lower energy of the excited state in the dppy–tpy complexes can be attributed to the cumulative effect of the lowering in energy of the acceptor ligand π^* orbitals upon increased delocalization across all three rings of the tpy ligand, compared to just two in **1**, and of the destabilized HOMO in the trans-configured complexes as discussed in the preceding section.

The absorption spectra of the dinuclear complexes are quite different from those of the monomers, with greatly enhanced absorption in the region 330–400 nm, which swamps the previously discernible band around 400 nm. This is no doubt due to the intense spin-allowed $^1\pi\text{-}\pi^*$ transitions associated with the oligo(phenylene) units that are anticipated in this region.⁴⁷

9. Emission. The new complexes are luminescent in solution at room temperature, $\lambda_{\text{max}} \sim 630 \text{ nm}$, displaying a single, structureless emission band in each case, typical of phosphorescence from excited states of primarily CT character. The excitation and emission spectra (at 298 and 77 K) of the parent complex **1** are shown in Figure 3. On the basis of the earlier discussion of the frontier orbitals, the emissive state is probably best regarded as having mixed $^3\text{d}(\text{Ir})/\pi(\text{N}^{\wedge}\text{C}^{\wedge}\text{N}) \rightarrow \pi^*(\text{N}^{\wedge}\text{N}^{\wedge}\text{C})$ character ($^3\text{MLCT/LLCT}$). The large blue shift in the emission maximum (2600 cm^{-1}) on cooling to 77 K in a rigid glass is typical of CT transitions, in which a considerable degree of molecular reorganization accompanies the formation of the excited state. The emission energy of **1** is similar to that of $[\text{Ir}(\text{ppy})_2(\text{bpy})]^+$ (Table 2), which also displays a similarly large thermally induced Stokes shift (2260 cm^{-1}).⁴⁸ On the other hand, the emission energy is substantially higher than that for the trans-C-configured complex

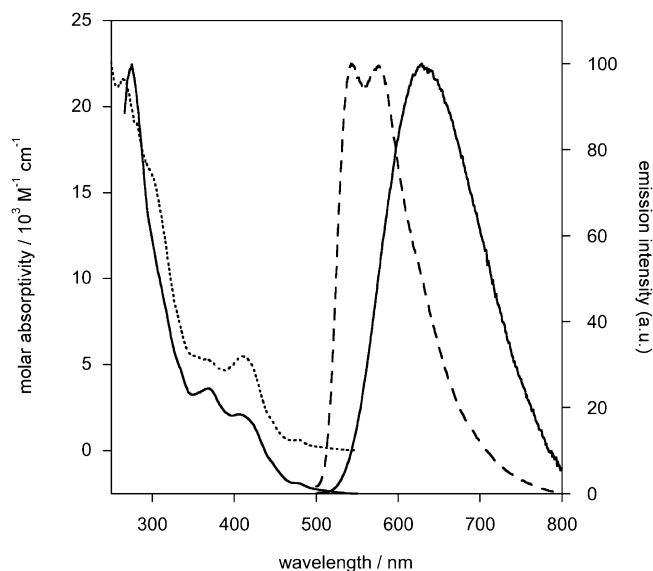


Figure 3. Emission and excitation spectra (solid lines) and absorption spectrum (dotted line, offset for clarity) of **1** in MeCN at 298 K ($\lambda_{\text{ex}} = 410 \text{ nm}$ and $\lambda_{\text{em}} = 600 \text{ nm}$, respectively; bandpasses = 3 nm). The emission spectrum at 77 K in an EPA glass is also shown (dashed line).

$[\text{Ir}(\text{tdppy})(\text{tpy}-\phi\text{-Br})]^+$ ($\lambda_{\text{max}} = 690 \text{ nm}$ ²³), mirroring the observations made for the absorption spectra.

The aryl substituents have a modest influence on the emission maximum, with a total variation in energy across the series of five complexes of 470 cm^{-1} (Figure 4 and Table 2). In principle, for an excited state of purely CT character, a linear correlation is anticipated between the energy of the CT excited state and the difference between the ground-state first-oxidation and first-reduction potentials ($\Delta E_{1/2}$) because the formation of the excited state formally involves oxidation of the HOMO and reduction of the LUMO.^{1,49} Using the trend in energy of the emission maxima as a guide to the trend in 0–0 energy of the excited state (an approximation that holds if the degree of reorganization is similar for each complex), this quantity can be plotted against $E_{1/2}^{\text{ox}} - E_{1/2}^{\text{red}}$, as shown in the inset to Figure 4. It can be seen that there is a close linear correlation for complexes **1–4**, supporting the CT assignment, but that complex **5** is anomalous in that it displays an emission energy lower than expected on the basis of the redox potentials. This is most probably due to the fact that the $E_{1/2}$ values, which relate to the ground state, underestimate the influence of the N^{^C^N} aryl substituent in the excited state. In the ground state, the pendent aryl group will be essentially orthogonal to the N^{^C^N} ligand owing to the flanking methyl groups, whereas the barrier to planarization is likely to be at least partially overcome upon formation of the excited state.

The luminescence lifetimes, τ , are in the range of 100–200 ns, which are reduced by a factor of 2–3 in an air-equilibrated solution. The luminescence quantum yield of the parent complex **1** is 0.023, similar to the value of 0.018 found for $[\text{Ir}(\text{ppy})_2(\text{bpy})]^+$.⁴⁸ The quantum yield increases slightly upon introduction of the pendent *p*-bromophenyl ring into the N^{^C^N} ligand and further to 0.063 for the biphenyl-appended

(46) Montalti, M.; Credi, A.; Prodi, L.; Gandolfi, M. T. *Handbook of Photochemistry*, 3rd ed.; CRC Press: Boca Raton, FL, 2006.

(47) Grimme, J.; Kreyenschmidt, M.; Uckert, F.; Mullen, K.; Scherf, U. *Adv. Mater.* **1995**, 7, 292.

(48) Glusac, K. D.; Jiang, S.; Schanze, K. S. *Chem. Commun.* **2002**, 2504.

(49) Cummings, S.; Eisenberg, R. *J. Am. Chem. Soc.* **1996**, 118, 1040.

Table 2. Luminescence Data for the Iridium Complexes, in CH₃CN Solution at 298 K except Where Stated Otherwise

complex ^a	emission $\lambda_{\text{max}}/\text{nm}$	$\Phi_{\text{lum}} \times 10^{2b}$ degassed (aerated)	τ/ns^c degassed (aerated)	$k_{\text{O}_2}/10^9$ $\text{M}^{-1} \text{s}^{-1}^d$	$k_{\text{r}}/10^5$ s^{-1}^e	$\Sigma k_{\text{nr}}/10^6$ s^{-1}^e	emission at 77 K ^f	
							$\lambda_{\text{max}}/\text{nm}$	$\tau/\mu\text{s}^c$
[Ir(ppy) ₂ (bpy)] ⁺	610 ^g	1.8 ^h	180 ^h		1.0 ^h	5.4 ^h	520 ⁱ	
[Ir(ppy) ₂ (tpy- ϕ -Br)] ⁺ ^j	690	3.5	1680 (198)	2.3	0.19	0.58	662 ^k	
[Ir(dpyx)(phbpy)] ⁺ (1)	632	2.3 (0.81)	120 (49)	6.4	1.9	8.1	544, 576	3.6
[Ir(dpyx)(mtbpy- ϕ -Br)] ⁺ (2)	639	2.8 (1.1)	130 (53)	5.9	2.2	7.5	556, 592	3.9
[Ir(dpyx)(mtbpy- ϕ -Ph)] ⁺ (3)	636	6.3 (2.5)	150 (57)	5.7	4.2	6.3	553, 590	4.0
[Ir(Brdpyx)(mtbpy- ϕ -Ph)] ⁺ (4)	625	4.8 (1.6)	190 (63)	5.6	2.5	5.0	544, 582	4.3
[Ir(Me ₂ -C ₆ H ₃ -dpyx)(mtbpy- ϕ -Ph)] ⁺ (5)	644	2.9 (1.2)	100 (47)	5.9	2.9	9.7	556, 593	3.5
[{Ir(dpyx) ₂ } ₂ μ -(mtbpy- ϕ -3-mtbpy)] ²⁺ (6)	632	2.7	140 (58)	5.3	1.9	7.0	565, 596	3.1, 68 ^l
[{Ir(dpyx) ₂ } ₂ μ -(mtbpy- ϕ -4-mtbpy)] ²⁺ (7)	633	2.7	144 (58)	5.4	1.9	6.8	577, 613	2.9, 72 ^l

^a Hexafluorophosphate salts in each case. ^b Luminescence quantum yield measured using [Ru(bpy)₃]Cl₂(aq) as the standard. ^c Lifetime registered at the emission maximum following excitation at 374 nm. ^d Bimolecular rate constant for quenching by O₂, estimated from τ values in degassed and aerated solutions. ^e Radiative (k_{r}) and nonradiative (Σk_{nr}) rate constants calculated from τ and ϕ values at 298 K. ^f In EPA glass. ^g In MeOH. ^h In degassed THF. ⁱ In 2-MeTHF. ^j Data from refs 23 and 24. ^k In 4:1 MeOH/EtOH. ^l Values estimated by fitting separately the short and long components of the decay.

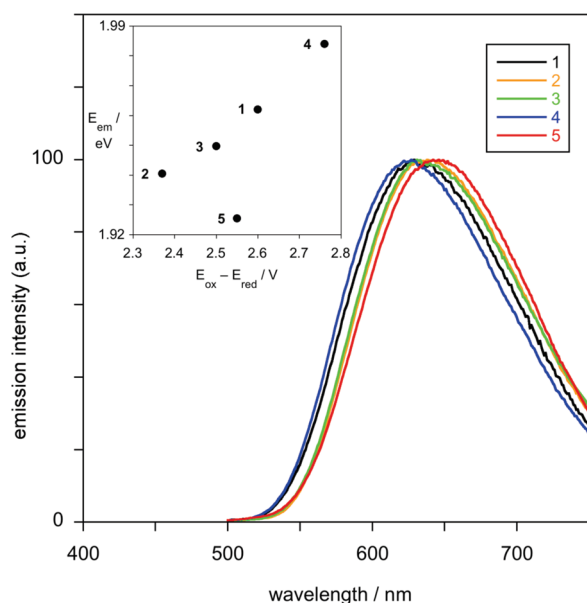


Figure 4. Emission spectra of iridium complexes **1–5** in a degassed acetonitrile solution at 298 K ($\lambda_{\text{ex}} = 410$ nm; excitation and emission bandpasses = 3 nm). Spectra shown are corrected and normalized to the same intensity; corresponding quantum yields are given in Table 2. Inset: plot of the emission energy (estimated from λ_{max}) as a function of the difference between the first oxidation and first reduction potentials.

complex **3**. Inspection of the radiative (k_{r}) and nonradiative (Σk_{nr}) decay rate constants (estimates of which are listed in Table 2, calculated from the experimentally determined τ and Φ values) reveals that the increase in the luminescence efficiency in going from complex **1** to **3** is due primarily to an increase in the radiative rate constant. In contrast, the introduction of an aryl substituent into the N^{^C^N} ligand (complex **5**) has a mildly detrimental effect owing to a small decrease in k_{r} and an increase in Σk_{nr} .

Comparison with the trans-cyclometalated [Ir(Ar'-dpp- γ)(Ar''-tpy)]⁺ complexes is instructive. Scandola et al. reported that they emit at substantially lower energy, $\lambda_{\text{max}} \sim 690$ nm, and were found to have unusually low radiative rate constants, $\sim 2 \times 10^4 \text{ s}^{-1}$,^{23,24} 1 order of magnitude lower than the values commonly found for cyclometalated iridium complexes, including those of the present work (Table 2). The low k_{r} was interpreted in terms of a high degree of LLCT character in the excited state, arising from the major

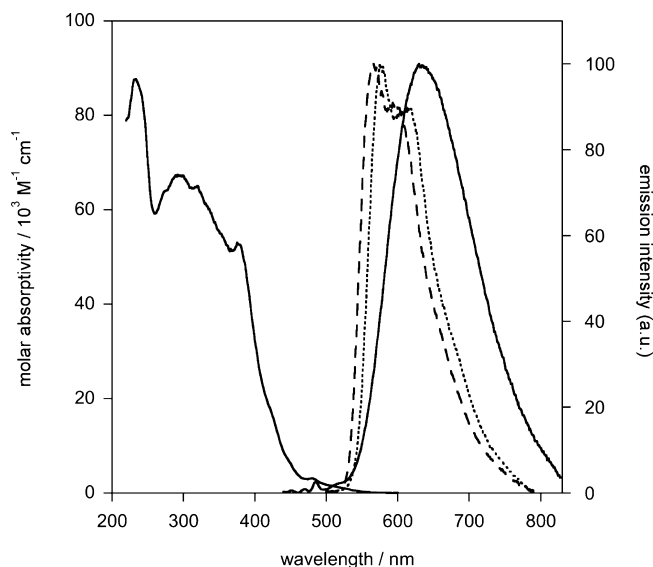


Figure 5. Absorption and room-temperature emission spectra of the dinuclear complex **6** (solid lines) in MeCN ($\lambda_{\text{ex}} = 380$ nm). The emission spectra of **6** and **7** in an EPA glass at 77 K are also shown (dashed and dotted lines, respectively).

contribution of the biscyclometalated dpp γ to the HOMO. In the present case, there is probably less LLCT character but rather a larger contribution of the metal to the HOMO, which is a key factor in determining the extent to which the formally forbidden triplet-to-singlet emissive transition is promoted.

The dinuclear complexes **6** and **7** are similarly luminescent in solution, displaying emission profiles, lifetimes, and quantum yields that are very similar to those of the parent complex **1** (Figure 5 and Table 2). At 77 K, however, some differences emerge. The emission is displaced to lower energy, with the effect being larger for the tetraphenyl bridge than the triphenyl: $\lambda_{\text{max}}^{\text{em}} = 544, 553, 565$, and 577 nm for **1**, **3**, **6**, and **7**, respectively. Moreover, the emission decay becomes biexponential for the dinuclear complexes (Figure 6). While the shorter component has a lifetime of around 3 μs , similar to that for all of the monometallic complexes and hence attributable to an excited state of similar CT character, the longer component (around 70 μs) is much longer than anticipated for an excited state with significant metal character. We suspect that this emission emanates from the

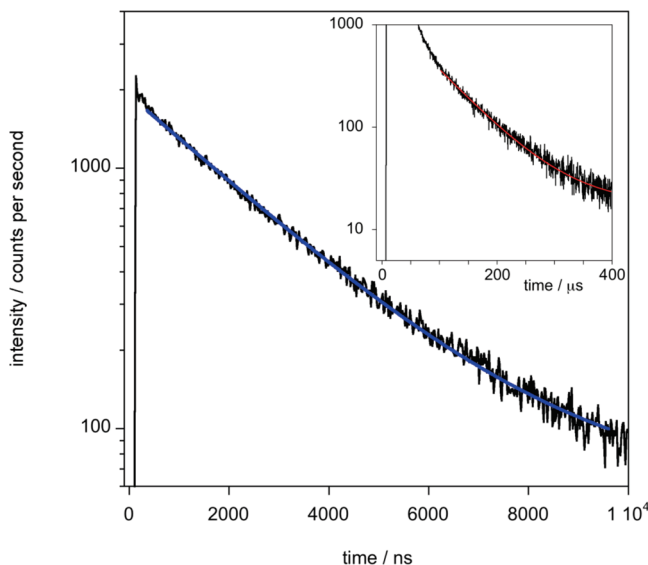


Figure 6. Decay kinetics of the dimetallic complex **7** in an EPA glass at 77 K registered at 600 nm ($\lambda_{\text{ex}} = 374$ nm). The estimated lifetime of the short component is 2.9 μs (blue fitted line to experimental data), while a value of 72 μs is obtained for the long component (red line and corresponding data, inset).

triplet π - π^* excited state associated with the bridging ligand. CT states are destabilized in a rigid matrix at 77 K, and so it is plausible that the CT and π - π^* states have similar energy at 77 K, leading to the two components observed, even though the former is unequivocally the lower at room temperature, which then ensures exclusively CT emission and monoexponential decay kinetics. A somewhat similar observation has been made by De Cola et al. for $[\{\text{Ir}(\text{F}_2\text{-ppy})_2\}_2\mu\text{-(bpy-}\phi\text{-bpy)}]^{2+}$ dinuclear complexes ($\phi = 3$ and 4).⁴¹ In that case, biexponential decay was observed even at room temperature. The difference probably arises from the fact that the CT states associated with the $\text{Ir}(\text{F}_2\text{ppy})(\text{bpy})^+$ units are higher in energy than those of the corresponding monometallic units in the present study.

10. Sensitization of Singlet Oxygen. The triplet states of many transition-metal complexes can act as sensitizers of singlet oxygen, O_2 $^1\Delta_{\text{g}}$, by energy transfer to the $^3\Sigma_{\text{g}}^-$ ground state of molecular oxygen. The quenching of the luminescence of **1** by dissolved oxygen was accompanied by the appearance of emission in the near-IR attributable to the formation and subsequent radiative decay of $^1\text{O}_2$, which emits ~ 1270 nm. The quantum yield of singlet oxygen formation by complex **1** under irradiation at 355 nm was determined using perinaphthenone as a standard,⁵⁰ giving a value of 0.4 ± 0.05 . No significant quenching of singlet oxygen by the complex was observed: the rate of decay of the $^1\text{O}_2$ emission in the near-IR was $1.67 \times 10^4 \text{ s}^{-1}$, essentially identical with the literature value of $1.64 \times 10^4 \text{ s}^{-1}$ in MeCN following production via standard sensitizers.⁵¹ This observation is also consistent with the observed photostability of the complex under irradiation in air-equilibrated solution and contrasts

with the previously reported instability of tricationic iridium(III) complexes, such as $[\text{Ir}(\text{bpy})_3]^{3+}$, to oxidative photochemical processes.⁵²

Previously, Thompson et al. have recorded $^1\text{O}_2$ quantum yields for a series of charge-neutral $[\text{Ir}(\text{N}^{\wedge}\text{C})_2(\text{L}^{\wedge}\text{X})]$ complexes, which were on the order of 0.6–1.0 in benzene.⁵³ Because cationic $[\text{Ir}(\text{N}^{\wedge}\text{C})_2(\text{N}^{\wedge}\text{N})]^+$ complexes have apparently not been investigated, we measured the $^1\text{O}_2$ quantum yield for $[\text{Ir}(\text{ppy})_2(\text{bpy})]^+$, which gave a value of 0.50, and for the trans-disposed carbon complex $[\text{Ir}(\text{dppy})(\text{tpy-}\phi\text{-CO}_2\text{Et})]^+$, for which a value of 0.60 was recorded. Thus, the values of the cationic complexes (0.4–0.6) are apparently consistently a little lower than those for the charge-neutral complexes.

Concluding Remarks

The new $[\text{Ir}(\text{N}^{\wedge}\text{C}^{\wedge}\text{N})(\text{N}^{\wedge}\text{N}^{\wedge}\text{C})]^+$ complexes are readily synthesized and display electrochemical and photophysical properties that are closely comparable to those of the well-established class of tris-bidentate complexes of which $[\text{Ir}(\text{N}^{\wedge}\text{C-ppy})_2(\text{N}^{\wedge}\text{N-bpy})]^+$ is the archetypal example. This contrasts with the chemistry of ruthenium(II), where the attractive excited-state properties of $[\text{Ru}(\text{bpy})_3]^{2+}$ are largely lost upon going to the bis-terdentate analogue $[\text{Ru}(\text{tpy})_2]^{2+}$, owing to increased nonradiative decay associated with low-lying metal-centered states. The achiral nature of the bis-terdentate iridium(III) systems avoids the problems associated with diastereoisomer formation that are encountered for the tris-bidentate complexes. Moreover, the present work reveals that the new complexes are particularly amenable to linear stepwise elaboration along the principal axis of the molecule, thanks to the ease with which the $\text{N}^{\wedge}\text{C}^{\wedge}\text{N}$ -coordinated ligand can be brominated, activating the molecule to cross-coupling reactions. By using appropriately substituted partners (e.g., boronic acids, stannanes, acetylides), incorporation of this attractive iridium core into larger conjugated assemblies will clearly be feasible.

Experimental Section

^1H and ^{13}C NMR spectra, including NOESY and COSY, were recorded on a Varian 500 MHz instrument. Chemical shifts (δ) are in parts per million, referenced to residual protiosolvent resonances, and coupling constants are in hertz. Electrospray ionization mass spectra were acquired on a time-of-flight Micromass LCT spectrometer. All solvents used in preparative work were at least Analar grade, and water was purified using the Purite system. Solvents used for optical spectroscopy were high-performance liquid chromatography grade. 1,3-Di(2-pyridyl)-4,6-dimethylbenzene (dpyxH),²⁹ 6-phenyl-2,2'-bipyridine (phbpyH),⁵⁴ and bis(μ -chloro)bis[1,3-di(2-pyridyl)-4,6-dimethylbenzene- N,C_2' , N' -iridium chloride] (**Ir**₂)²⁸ were prepared as described previously. The synthesis and characterization of mtbpyH- ϕ -Br are described in the Supporting Information.

$[\text{Ir}(\text{N}^{\wedge}\text{C}^{\wedge}\text{N-dpyx})(\text{N}^{\wedge}\text{N}^{\wedge}\text{C-phbpy})](\text{PF}_6)$ (1**).** A suspension of **Ir**₂ (50 mg, 0.048 mmol), phbpyH (25 mg, 0.11 mmol), and silver(I)

(50) Schmidt, R.; Tanielian, C.; Dunsbach, R.; Wolff, C. *J. Photochem. Photobiol. A* **1994**, 79, 11.

(51) Clennan, E. L.; Noe, L. J.; Wen, T.; Szneler, E. *J. Org. Chem.* **1989**, 54, 3581.

(52) Demas, J. N.; Harris, E. W.; McBride, R. P. *J. Am. Chem. Soc.* **1977**, 99, 3547.

(53) Gao, R.; Ho, D. G.; Hernandez, B.; Selke, M.; Murphy, D.; Djurovich, P. I.; Thompson, M. E. *J. Am. Chem. Soc.* **2002**, 124, 14828.

(54) Kröhnke, F. *Synthesis* **1976**, 1.

trifluoromethanesulfonate (58 mg, 0.23 mmol) in ethylene glycol (4 mL) was stirred at room temperature under N₂ for 1 h and then heated to 196 °C for a further 3 h. After cooling to room temperature, the precipitated AgCl was collected by centrifuge and washed with acetonitrile (2 × 2 mL). The acetonitrile and ethylene glycol solutions were combined and added to a saturated aqueous KPF₆ solution (20 mL). The resulting yellow/orange precipitate was collected by centrifuge, washed with water (3 × 5 mL), and dried under vacuum. Purification by flash column chromatography (silica, CH₂Cl₂/MeOH, gradient elution from 100/0 to 99/1) gave the desired product as a yellow/orange solid (61 mg, 78%). ¹H NMR (acetone-*d*₆, 500 MHz): δ 8.72 (1H, d, ³J = 8.0, H³-NNC), 8.70 (1H, d, ³J = 8.0, H^{3'}-NNC), 8.54 (1H, d, ³J = 8.5, H^{5'}-NNC), 8.38 (1H, t, ³J = 8.0, H^{4'}-NNC), 8.31 (2H, d, ³J = 8.5, H³-NCN), 8.10 (1H, td, ³J = 8.0, ⁴J = 1.5, H⁴-NNC), 7.86 (1H, d, ³J = 7.5, H^{3''}-NNC), 7.83 (2H, td, ³J = 8.0, ⁴J = 1.5, H⁴-NCN), 7.68 (2H, d, ³J = 5.5, H⁶-NCN), 7.65 (1H, d, ³J = 5.0, H⁶-NNC), 7.39 (1H, t, ³J = 7.0, H⁵-NNC), 7.21 (1H, s, H^{4'}-NCN), 6.95 (2H, t, ³J = 7.0, H⁵-NCN), 6.85 (1H, t, ³J = 7.5, H^{4''}-NNC), 6.62 (1H, td, ³J = 7.5, ³J = 1.0, H^{5''}-NNC), 5.94 (1H, d, ³J = 7.5, H^{6''}-NNC), 2.97 (6H, s, Me). ¹³C NMR (acetone-*d*₆, 500 MHz): δ 150.9 (C⁶-NCN), 138.4 (C⁴-NCN), 130.0 (C^{4'}-NCN), 123.7 (C⁵-NCN), 122.6 (C³-NCN), 120.4 (C^{3'}). MS (ES⁺): *m/z* 681.3 [M]⁺. HRMS (ES⁺): Found: *m/z* 681.17581 for [M]⁺. Calcd for ¹⁹¹IrC₃₄H₂₆F₆N₄: *m/z* 681.17580. Elem anal. Calcd for C₃₄H₂₆F₆IrN₄P: C, 49.4; H, 3.2; N, 6.8. Found: C, 48.8; H, 3.4; N, 6.7. One spot by thin-layer chromatography (TLC; silica): *R*_f = 0.43 in dichloromethane/methanol (90:10).

1-Br₂. ¹H NMR and mass spectrometric data for the dibrominated complex **1-Br₂** are recorded in the Supporting Information.

[Ir(N[^]C[^]N-dpyx)(N[^]N[^]C-mtbp-φ-Br)](PF₆) (2). A suspension of Ir₂ (52 mg, 0.050 mmol), mtbpH-φ-Br (41 mg, 0.10 mmol), and silver(I) trifluoromethanesulfonate (80 mg, 0.31 mmol) in ethylene glycol (3 mL) was stirred at room temperature for 1 h under a N₂ atmosphere. The suspension was then stirred and heated to 196 °C under N₂ for a further 2 h. After cooling to room temperature, an orange precipitate formed. The solids were collected by centrifuge, and an orange product was extracted into acetonitrile (5 mL), leaving a gray residue of AgCl. The acetonitrile and ethylene glycol solutions were combined and reduced in volume, before being added to a saturated aqueous KPF₆ solution (25 mL). The resulting orange precipitate was collected by centrifuge, washed with water (3 × 5 mL), and dried under vacuum. Purification by flash column chromatography (silica, CH₂Cl₂/MeOH, gradient elution from 100:0 to 98.75:1.25) gave the desired product as an orange solid (84 mg, 84%). ¹H NMR (acetone-*d*₆, 500 MHz): δ 9.05 (1H, d, ⁴J = 2.0, H^{3'}-NNC), 8.95 (1H, d, ³J = 8.0, H-NNC), 8.88 (1H, d, ⁴J = 1.0, H^{5'}-NNC), 8.32 (2H, d, ³J = 8.0, H³-NCN), 8.21 (2H, d, ³J = 8.5, H^b), 8.13 (1H, td, ³J = 8.0, ⁴J = 1.5, H⁴-NNC), 7.90 (3H, m, H^{3'}-NNC, H^a), 7.83 (2H, td, ³J = 8.0, ⁴J = 1.5, H⁴-NCN), 7.76 (2H, dd, ³J = 6.0, ⁴J = 1.0, H⁶-NCN), 7.68 (1H, d, ³J = 5.0, H⁶-NNC), 7.41 (1H, ddd, ³J = 8.5, ³J = 7.0, ⁴J = 1.0, H^{5''}-NNC), 7.21 (1H, s, H^{4'}-NCN), 6.94 (2H, td, ³J = 7.5, ⁴J = 1.0, H⁵-NCN), 6.49 (1H, d, ³J = 7.5, H⁵-NNC), 5.83 (1H, d, ³J = 8.0, H^{6''}-NNC), 2.97 (6H, s, Me-NCN), 2.16 (3H, s, Me-NNC). MS (MALDI, DCTB matrix): *m/z* 851.3 [M]⁺. HRMS (ES⁺): Calcd for ¹⁹¹IrC₄₁H₃₁N₄⁷⁹Br: *m/z* 849.13326. Found: *m/z* 849.13533 [M]⁺. Elem anal. Calcd for C₄₁H₃₁BrF₆IrN₄P: C, 49.5; H, 3.1; N, 5.6. Found: C, 49.0; H, 3.5; N, 6.3. One spot by TLC (silica) *R*_f = 0.65 in dichloromethane/methanol (90:10).

[Ir(N[^]C[^]N-dpyx)(N[^]N[^]C-mtbp-φ-Ph)](PF₆) (3). A mixture of iridium complex **2** (32 mg, 0.032 mmol), phenylboronic acid (7.8 mg, 0.064 mmol), and sodium carbonate (10 mg, 0.096 mmol) in 100 μL water) in dimethyl sulfoxide (5 mL) was degassed by

three freeze–pump–thaw cycles. Tetrakis(triphenylphosphine)-palladium(0) (4.4 mg, 0.0038 mmol) was added under a positive pressure of N₂. The resultant orange suspension was stirred at 80 °C under a N₂ atmosphere for 18 h. The mixture was cooled to room temperature, diluted with acetonitrile (1 mL), and filtered to remove the insoluble palladium black that had formed. The filtrate was added to a saturated aqueous KPF₆ solution (25 mL); the resultant orange precipitate was collected by a centrifuge, washed with water (10 × 3 mL), and dried under vacuum. Purification by flash column chromatography (silica, CH₂Cl₂/MeOH, gradient elution from 100:0 to 99:1) gave the desired product as an orange solid (49 mg, 72%). ¹H NMR (acetone-*d*₆, 500 MHz): δ 9.10 (1H, d, ⁴J = 1.0, H^{3'}-NNC), 9.00 (1H, dd, ³J = 13.5, ³J = 7.5, H^{3''}-NNC), 8.93 (1H, d, ⁴J = 1.0, H^{5'}-NNC), 8.35 (4H, m, H^b- and H³-NCN), 8.14 (1H, td, ³J = 7.5, ⁴J = 1.5, H⁴-NNC), 8.02 (2H, d, ³J = 8.0, H^a), 7.97 (1H, s, H³-NNC), 7.84 (4H, m, H⁴-NCN, H^b), 7.79 (2H, d, ³J = 6.0, H⁶-NCN), 7.68 (1H, d, ³J = 4.5, H⁶-NNC), 7.56 (2H, t, ³J = 7.5, H^a), 7.46 (1H, t, ³J = 7.5, H^c), 7.42 (1H, dd, ³J = 7.0, ³J = 5.5, H⁵-NNC), 7.22 (1H, s, H^{4'}-NCN), 6.96 (2H, td, ³J = 6.5, ⁴J = 1.0, H^{5''}-NCN), 6.50 (1H, d, ³J = 7.5, H⁵-NNC), 5.84 (1H, d, ³J = 7.5, H^{6''}-NNC), 2.98 (6H, s, Me-NCN), 2.17 (3H, s, Me-NNC). MS (MALDI, DCTB matrix): *m/z* 849.4 [M]⁺. HRMS (ES⁺): Calcd for ¹⁹¹IrC₄₇H₃₆N₄: *m/z* 847.25405. Found: *m/z* 847.25409 [M]⁺. Elem anal. Calcd for C₄₇H₃₆IrN₄P: C, 56.9; H, 3.7; N, 5.6. Found: C, 56.6; H, 3.7; N, 5.4. One spot by TLC (silica) *R*_f = 0.51 in dichloromethane/methanol (90:10).

[Ir(N[^]C[^]N-Brdpyx)(N[^]N[^]C-mtbp-φ-Ph)](PF₆) (4). A mixture of iridium complex **3** (29 mg, 0.029 mmol) and *N*-bromosuccinimide (NBS; 5.2 g, 0.029 mmol) was stirred in acetonitrile (2 mL) for 20 h, during which some precipitation of an orange solid was observed. Additional acetonitrile (2 mL) was added to fully dissolve the product. The solution was then added to a saturated aqueous KPF₆ solution (20 mL), giving a precipitate, which was collected by centrifuge, washed with water (3 × 5 mL), and dried under vacuum to give the product as an orange solid (31 mg, 100%). ¹H NMR (acetone-*d*₆, 500 MHz): δ 9.13 (1H, s, H^{3'}-NNC), 9.04 (1H, t, ³J = 8.5, H^{3''}-NNC), 8.96 (1H, s, H^{5'}-NNC), 8.46 (2H, d, ³J = 8.5, H³-NCN), 8.38 (2H, d, ³J = 8.5, H^b), 8.17 (1H, t, ³J = 7.0, H⁴-NNC), 8.05 (2H, d, ³J = 8.0, H^a), 8.00 (1H, s, H³-NNC), 7.92 (2H, t, ³J = 6.5, H⁴-NCN), 7.87 (4H, m, H^b- and H⁶-NCN), 7.77 (1H, d, ³J = 5.5, H⁶-NNC), 7.58 (2H, t, ³J = 7.5, H^a), 7.49 (1H, t, ³J = 7.5, H^c), 7.43 (1H, t, ³J = 7.5, H^{5''}-NNC), 7.05 (2H, t, ³J = 7.5, H⁵-NCN), 6.53 (1H, d, ³J = 7.0, H⁵-NNC), 5.86 (1H, d, ³J = 8.0, H^{6''}-NNC), 3.22 (6H, s, Me-NCN), 2.20 (3H, s, Me-NNC). MS (MALDI, DCTB matrix): *m/z* = 927.3 [M]⁺. HRMS (ES⁺): Calcd for ¹⁹¹IrC₄₇H₃₅N₄⁷⁹Br: *m/z* 925.16456. Found: *m/z* 925.16344. Elem anal. Calcd for C₄₇H₃₅BrF₆IrN₄P: C, 52.8; H, 3.3; N, 5.2. Found: C, 52.3; H, 3.6; N, 4.8. One spot by TLC (silica) *R*_f = 0.53 in dichloromethane/methanol (90:10).

[Ir(N[^]C[^]N-Me₂C₆H₃-dpyx)(N[^]N[^]C-mtbp-φ-Ph)](PF₆) (5). A mixture of the brominated iridium complex **4** (35 mg, 0.035 mmol), 3,5-dimethylphenylboronic acid (10 mg, 0.070 mmol), and sodium carbonate (12 mg, 0.11 mmol in 100 μL water) in dimethyl sulfoxide (5 mL) was degassed by three freeze–pump–thaw cycles. Tetrakis(triphenylphosphine)palladium(0) (4.9 mg, 0.0042 mmol) was added under a positive pressure of N₂. The resultant orange suspension was stirred at 80 °C under N₂ for 18 h. The dimethyl sulfoxide solution was cooled to room temperature, diluted with acetonitrile (2 mL), and filtered to remove the insoluble palladium black that had formed. The filtrate was added to a saturated aqueous KPF₆ solution (25 mL); the resultant orange precipitate was collected by centrifuge, washed with water (3 × 5 mL), and dried under vacuum. Purification by flash column chromatography (silica,

CH₂Cl₂/MeOH, gradient elution from 100:0 to 99.1:0.9) gave the desired product as an orange solid (20 mg, 53%). ¹H NMR (acetone-*d*₆, 500 MHz): δ 9.12 (1H, d, ⁴*J* = 1.0, H^{3'}-NNC), 9.02 (1H, d, ³*J* = 8.5, H^{3''}-NNC), 8.94 (1H, d, ⁴*J* = 1.0, H^{5'}-NNC), 8.37 (4H, m, H^b-NNC and H³-NCN), 8.16 (1H, td, ³*J* = 8.0, ⁴*J* = 1.5, H⁴-NNC), 8.03 (2H, d, ³*J* = 8.5, H^a), 7.99 (1H, s, H³-NNC), 7.83 (6H, m, H^b, H⁴-NCN, and H⁶-NCN), 7.76 (1H, d, ³*J* = 5.0, H⁶-NNC), 7.56 (2H, t, ³*J* = 7.5, H^a), 7.45 (2H, m, H^c and H^{5''}-NNC), 7.16 (1H, s, H^c), 7.07 (1H, s, H^b-NCN or H^d), 7.02 (1H, s, H^b-NCN or H^d), 6.97 (2H, td, ³*J* = 6.0, ⁴*J* = 1.5, H⁵-NCN), 6.55 (1H, d, ³*J* = 8.5, H⁵-NNC), 5.95 (1H, d, ³*J* = 8.0, H^{6''}-NNC), 2.66 (6H, s, Me-NCN), 2.46 (6H, d, ⁴*J* = 3.5, Me-NCN-pendent), 2.19 (3H, s, Me-NNC). MS (MALDI, DCTB matrix): *m/z* 953.4 [M]⁺. HRMS (ES⁺). Calcd for ¹⁹¹IrC₅₅H₄₄N₄: *m/z* 951.31665. Found: *m/z* 951.31694 [M]⁺. Elem anal. Calcd for C₅₅H₄₄F₆IrN₄P: C, 60.3; H, 4.1; N, 5.1. Found: C, 59.9; H, 3.9; N, 5.7. One spot by TLC (silica) *R*_f = 0.48 in dichloromethane/methanol (90:10).

[{Ir(N⁴C⁴N-dpyx)₂]₂μ-(N⁴N⁴C-mtbp-*(φ)*₃-N⁴N⁴C-mtbp-*(φ)*)](PF₆)₂ (6). A mixture of complex **2** (60 mg, 0.060 mmol), 1,4-benzenediboronic acid (6 mg, 0.036 mmol), and sodium carbonate (9.5 mg, 0.09 mmol in 100 μL water) in dimethyl sulfoxide (5 mL) was degassed by three freeze–pump–thaw cycles. The catalyst Pd(PPh₃)₄ (4.2 mg, 0.0036 mmol) was added under a positive pressure of N₂. The resulting orange suspension was stirred at 80 °C under a N₂ atmosphere for 18 h. Upon cooling to room temperature, the mixture was diluted with acetonitrile (2 mL) and filtered to remove the insoluble palladium black that had formed. The filtrate was added to a saturated KPF₆ solution (25 mL), and the orange precipitate that formed was collected by centrifuge, washed with water (3 × 5 mL), and dried under vacuum. Purification by flash column chromatography (silica, acetonitrile/water/saturated KNO₃ solution, gradient elution from 100:0:0 to 95:4.95:0.05) gave the desired product as an orange solid (23 mg, 30%). ¹H NMR (CD₃CN, 500 MHz): δ 8.79 (2H, s, H^{3'}), 8.71 (2H, s, H^{5'}), 8.67 (2H, d, ³*J* = 8.0, H³-NNC), 8.32 (4H, d, ³*J* = 8.0, H^b), 8.26 (4H, d, ³*J* = 8.0, H³-NCN), 8.16 (4H, d, ³*J* = 8.0, H^a-NNC), 8.07 (4H, s, H^b), 8.03 (2H, t, ³*J* = 7.0, H⁴-NNC), 7.90 (2H, s, H^{3''}), 7.78 (4H, t, ³*J* = 7.5, H⁴-NCN), 7.61 (4H, d, ³*J* = 6.0, H⁶-NCN), 7.56 (2H, d, ³*J* = 5.5, H⁶-NNC), 7.28 (2H, t, ³*J* = 6.5, H⁵), 7.21 (2H, s, H^{4'}-NCN), 6.89 (4H, t, ³*J* = 6.5, H⁵-NCN), 6.57 (2H, d, ³*J* = 9.0, H^{5''}), 5.82 (2H, d, ³*J* = 7.5, H^{6''}), 2.96 (12H, s, Me-NCN), 2.46 (6H, s, Me-NNC). MS (MALDI, DCTB matrix): *m/z* 1765.4 [M + PF₆]⁺, 1620.4 [M + e⁻]⁺. Experimental isotope patterns match the theoretical simulation (see the Supporting Information). One spot by TLC (silica) *R*_f = 0.51 in an acetonitrile/water/saturated KNO₃ solution (90:9.8:0.2).

[{Ir(N⁴C⁴N-dpyx)₂]₂μ-(N⁴N⁴C-mtbp-*(φ)*₄-N⁴N⁴C-mtbp-*(φ)*)](PF₆)₂ (7). This dimeric complex was prepared in the same way and on the same molar scale as **6**, but using 4,4'-biphenyldiboronic acid (8.7 mg, 0.036 mmol) in place of benzenediboronic acid. Purification of the hexafluorophosphate salt by flash column chromatography (silica, acetonitrile/water/saturated KNO₃ solution, gradient elution from 100:0:0 to 95:4.95:0.05) gave the desired product as an orange solid (0.021 g, 35%). ¹H NMR (CD₃CN, 700 MHz): δ 8.78 (2H, s, H^{3'}), 8.70 (2H, s, H^{5'}), 8.66 (2H, d, ³*J* = 7.0, H³-NNC), 8.30 (4H, d, ³*J* = 7.7, H^b), 8.26 (4H, d, ³*J* = 7.7, H³-NCN), 8.14 (4H, d, ³*J* = 7.7, H^a), 8.04–8.00 (10H, m, H⁴-NNC, H^b, H^a), 7.89 (2H, s, H^{3''}-NNC), 7.78 (4H, t, ³*J* = 7.0, H⁴-NCN), 7.61 (4H, d, ³*J* = 6.3, H⁶-NCN), 7.55 (2H, d, ³*J* = 6.3, H⁶-NNC), 7.27 (2H, t, ³*J* = 7.0, H⁵-NNC), 7.21 (2H, s, H^{4'}-NCN), 6.89 (4H, t, ³*J* = 6.3, H⁵-NCN), 6.57 (2H, d, ³*J* = 8.4, H^{5''}), 5.82 (2H, d, ³*J* = 8.4, H^{6''}), 2.96 (12H, s, Me-NCN), 2.25 (6H, s, Me-NNC). MS (MALDI, DCTB matrix): *m/z* 1841.4 [M + PF₆]⁺. Experimental

isotope patterns match the theoretical simulation (see the Supporting Information). One spot by TLC (silica) *R*_f = 0.57 in an acetonitrile/water/saturated KNO₃ solution (90:9.8:0.2).

Photophysical Measurements. Absorption spectra were measured on a Biotek Instruments XS spectrometer, using quartz cuvettes of 1 cm path length. Steady-state luminescence spectra were measured using a Jobin Yvon FluoroMax-2 spectrofluorimeter, fitted with a red-sensitive Hamamatsu R928 photomultiplier tube (PMT); the spectra shown are corrected for the wavelength dependence of the detector, and the quoted emission maxima refer to the values after correction. Samples for emission measurements were contained within quartz cuvettes of 1 cm path length modified with appropriate glassware to allow connection to a high-vacuum line. Degassing was achieved via a minimum of three freeze–pump–thaw cycles while connected to the vacuum manifold; the final vapor pressure at 77 K was <5 × 10⁻² mbar, as monitored using a Pirani gauge. Luminescence quantum yields were determined by the method of continuous dilution, using [Ru(bpy)₃]Cl₂ in an air-equilibrated aqueous solution as the standard (ϕ = 0.028⁵⁵); the estimated uncertainty in ϕ is ±20% or better.

The luminescence lifetimes of the complexes were measured by time-correlated single-photon counting (TCSPC), following excitation at 374.0 nm with an EPL-375 pulsed-diode laser. The emitted light was detected at 90° using a Peltier-cooled R928 PMT after passage through a monochromator. The estimated uncertainty in the quoted lifetimes is ±10% or better. For the dimetallic complexes **6** and **7**, an estimate of the short component of the decay was made in this way using TCSPC, while the longer component was analyzed using multichannel scaling following excitation by a pulsed xenon lamp. Bimolecular rate constants for quenching by molecular oxygen, *k*_Q, were determined from the lifetimes in a degassed and air-equilibrated solution, taking the concentration of oxygen in CH₃CN at 0.21 atm of O₂ to be 1.9 mmol dm⁻³.⁴⁶

The quantum yields of singlet oxygen production were obtained by measuring the intensity of the ¹O₂ near-IR luminescence in an air-saturated MeCN solution and comparing it with that measured for a solution of perinaphthenone {1-*H*-phenanthrene-1-one, Φ(¹O₂) = 0.95⁵⁰} of the same optical density (<0.2). The samples were excited at 355 nm using the third harmonic of a Nd:YAG laser, and the emission in the near-IR was detected using a liquid-N₂-cooled germanium photodiode detector. A filter was used to eliminate light of <1100 nm. Measurements at a range of incident light powers were made and the quantum yields determined from the ratio of the gradients of intensity versus power for the sample and standard. Representative plots are shown in the Supporting Information.

Acknowledgment. We thank EPSRC and the University of Durham for the award of a DTA studentship to V.L.W. and Frontier Scientific Ltd. for their valued help in supplying key reagents. We are indebted to Dr. Supiah Navaratnam and Dr. Ruth Edge for their assistance in measuring ¹O₂ quantum yields, carried out with support from CCLRC Daresbury Laboratory.

Supporting Information Available: Syntheses, ¹H NMR and MS data, DFT calculations, frontier orbitals, singlet oxygen quantum yields, and a complete reference for *Gaussian*. This material is available free of charge via the Internet at <http://pubs.acs.org>.

IC701788D

(55) Nakamaru, K. *Bull. Chem. Soc. Jpn.* **1982**, *55*, 2697.